Hyperfine Interact (2016) 237: 21
DOI 10.1007/s10751-016-1227-3

Quantum-mechanical and continual models of magnetic dynamics for antiferromagnetic particles in Mössbauer spectra analysis

I. Mischenko[1] · **M. Chuev**[1]

Published online: 18 February 2016

Abstract A standard multi-level relaxation model of magnetic dynamics of single-domain particles together with recently developed quantum-mechanical and continual models of specific thermo- and magnetic dynamics of antiferromagnetic particles were applied to analyse temperature series of Mössbauer spectra of Fe_2O_3 based nanoparticles. Advantages of these models, their comparison and further generalizations are discussed on the example of the particular experimental data.

Keywords Mössbauer spectroscopy · Antiferromagnetic particles · Maghemite · Hematite · Magnetic dynamics · Thermodynamics

1 Introduction

Along with the progress in nanotechnology the sphere of application of iron oxides magnetic nanoparticles continues to broaden. These materials are widespread in nature, easily synthesizable under industrial and laboratory conditions, and also nontoxic; this allows us to use them as working bases for biological and medical purposes. Extension of the sphere of application of magnetic nanomaterials requires further improvement in the methods of their diagnostics, which is a challenging scientific and technical problem. Electron microscopy allows us to control sizes and shapes of synthesized particles, but it is insensitive to the chemical composition and magnetic ordering of the obtained substances. X-ray methods, though widely used to characterize bulk materials, often provide little information on finely dispersed powders due to the strong broadening of diffraction peaks from nanosize grains.

This article is part of the Topical Collection on *Proceedings of the International Conference on the Applications of the Mössbauer Effect (ICAME 2015), Hamburg, Germany, 13–18 September 2015*

✉ I. Mischenko
IlyaMischenko@rambler.ru

[1] Institute of Physics and Technology, Russian Academy of Sciences, 117218 Moscow, Russia

Chemical (and in particularly histological) methods allow us to establish the presence of iron of a specific valence, but they cannot answer the question of the quantitative content of one or another phase.

In this connection high-resolution Mössbauer spectroscopy, which has been successfully used to study both bulk and nanocrystalline materials for the last half century, takes on special significance. First of all, the record narrow width of the resonance line allows us to determine intra-atomic and crystalline fields, and therefore the valences of absorbing atoms and their chemical environment, so that the spectral contributions from different compounds can be separated and used to estimate the concentrations of corresponding phases. Second, the specific distributions of the hyperfine parameters that appear upon moving from bulk samples to nanocrystallites, together with the short decay time of the excited state of the nucleus, provide us good insight into the size and dynamic effects inherited to the systems of small particles. Finally, sensitivity of Mössbauer spectroscopy to local fields on nuclei, in contrast to macroscopic characteristics averaged over a sample makes it a powerful tool for study magnetic structure of matter. However, to extract the rich information from the experimental Mössbauer spectra of magnetic nanocomposites, adequate theoretical models considering the specific thermodynamic and magnetic properties of studied systems must be developed.

In the last years we have developed the formalism applicable to describe Mössbauer spectra of both ferromagnetic [1–3] and antiferromagnetic [4–6] particles, and the main goal of this contribution is to show the efficiency of the new approaches by the example of diagnostics of trivalent iron oxide nanoparticles.

2 Experiment and standard analysis

The details of synthesis of iron oxide nanocrystals in a dextran shell was described in [7], which was dedicated to their complex experimental investigation via electron microscopy, magnetometry, NMR and Mössbauer spectroscopy. The first aim for the researchers was to create very small and at that monodisperse particles, and the transmission electron microscopy data, which found a narrow spread of diameters of magnetic nuclei close to 3 nm, indicates the authors of [7] reached their purpose. After that the scientists focused on the magnetic behavior of an ensemble of synthesized ultrafine particles. Supposing initially that they were dealing with ferrimagnetic crystals of maghemite γ-Fe_2O_3, the authors of [7] interpreted the evolution of the Mössbauer spectra from a well-resolved magnetic sextet at low temperatures to a clearly pronounced quadrupole doublet at high temperatures as a relaxation transition from the frozen-in spin state to the superparamagnetic state. In the same way they treated direct measurements of magnetic susceptibility in dc and ac fields along with indirect data on the nuclear magnetic resonance on hydrogen atoms in a polymer shell. The difficulties of such description and deviations in the behavior of the system from the expected type were attributed to the presence in the particles a disordered outer layer and to the effect of interparticle interaction.

Desiring to verify their conclusions, the authors of [7] turned to us with a proposal to perform a quantitative analysis of their Mössbauer data kindly putting them at our disposal. These data, partly published in the mentioned article, are presented in Fig. 1. As the theoretical basis for simultaneous analysis of the temperature series of the spectra we chose the standard multilevel model of magnetic dynamics of single-domain particles [1], generalized for the presence of quadrupole interaction on the nuclei [2]. Besides usual characteristics of hyperfine interactions as contact Coulomb interaction δ, magnetic dipole interaction H_{hf}

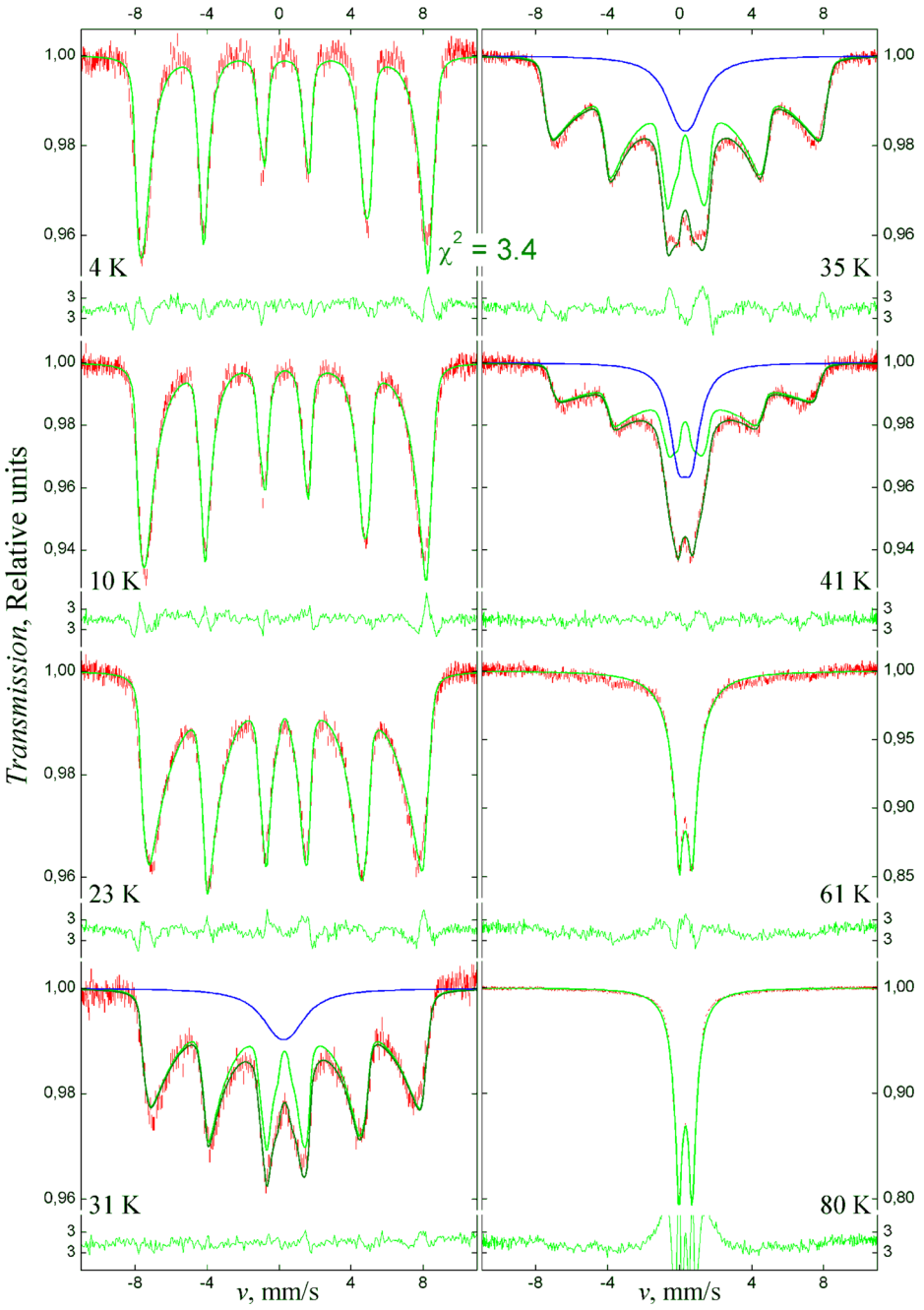

Fig. 1 Experimental Mössbauer spectra of Fe_2O_3 nanoparticles at different temperatures, corrected for the absorber thickness (*red bars*), and theoretical spectra (*green lines*) calculated in the multi-level model of magnetic dynamics of single-domain particles with an additional contribution from weakly magnetic states (*blue lines*) as well as total spectra (*dark-green lines*). Relative discrepancy between theory and experiment is shown on the small insertions

Table 1 Parameters of Fe_2O_3 nanoparticles at different temperatures T, derived from the experimental Mössbauer spectra using the multi-level model of magnetic dynamics of single-domain particles with an additional contribution from weakly magnetic states: quadrupolar shift q shared for both components and all temperatures, diffusion constant D, anisotropy energy barrier KV, hyperfine field H_{hf}, isomer shifts δ and δ_a and effective absorber thicknesses σ and σ_a for the main and additional components, respectively, as well as total line width for additional doublet Γ_a

T, K	4	10	23	31	35	41	61	80
q, mm/s	0.3655 (3)							
D, mm/s	0						10.3 (1)	16.3 (1)
KV, K	38.2 (7)	69.9 (7)	78.7 (4)	73.2 (17)	55.9 (8)	40.3 (16)	0	
H_{hf}, kOe	507.7 (3)	502.0 (2)	491.4 (2)	486.8 (5)	484.6 (3)	460.9 (8)	430	400
δ, mm/s	0.326 (3)	0.330 (2)	0.336 (2)	0.322 (5)	0.340 (3)	0.366 (7)	0.340 (2)	0.3265(4)
σ	2.84 (2)	3.06 (1)	2.95 (1)	2.34 (2)	2.51 (1)	2.04 (1)	2.59 (1)	2.822 (2)
δ_a, mm/s				0.25 (5)	0.32 (1)	0.30 (1)		
Γ_a, mm/s				2.4 (2)	1.9 (1)	1.2 (1)		
σ_a				0.33 (1)	0.47 (1)	0.76 (1)		

Mean-square errors in the last digit are shown in brackets

and electric quadrupole interaction q, this model takes into account all electronic states of a single-domain particle with volume V and spin S in the macroscopic potential well with the energy density

$$E(\theta) = -K\cos^2\theta, \tag{1}$$

where K is the magnetic anisotropy constant and θ is the angle between the easy axis and the magnetization vector of the particle, so that its stationary levels are

$$E_m = -Km^2/S(S+1), \tag{2}$$

where $m = -S, -S+1, \ldots, S$ are particle's spin projections onto the easy axis. The populations of the levels are determined by the Boltzmann distribution

$$W_m \sim \exp(-E_m V/k_B T), \tag{3}$$

where k_B is Boltzmann constant and T is absolute temperature, and the relaxation process in this model is specified by the diffusion constant D, so that energy independent part of the transition probability between adjacent states is

$$p_{m\,m\pm1} = D\,[S(S+1) - m(m\pm1)], \tag{4}$$

whereas its energy dependence is given by the multiplier

$$f_{m\,m\pm1} = \min(1,\ W_{m\pm1}/W_m). \tag{5}$$

The results of fit in this model are presented in Fig. 1, and the found values of parameters are placed in Table 1. However, our analysis shows that the standard relaxation model is not enough to describe all of the spectra even upon actually independent processing: though the low-temperature measurements can be explained in terms of the chosen approach if we allow some temperature variation in the of anisotropy energy KV and the high-temperature slightly resolved structure can be formally ascribed to a sharp increase in diffusivity D, the shape of the experimental curves in the intermediate temperature range does not keep within the selected theoretical scheme and requires involving an additional central component. This contribution is shown in Fig. 1 by an extra doublet of broadened lines with splitting $2q$,

and its parameters are presented in Table 1. Though found values of isomer shift and hyperfine field are typical for maghemite, observable large strength of quadrupolar interaction is unusual for this compound, which is characterized by practically zero value of EFG on iron nuclei [8]. Moreover, the relaxation in most cases turns out to play no significant role ($D = 0$) and some signs of the resolved magnetic structure survive even in high temperature spectra, which indicates that they are not caused by relaxation processes. It is worth mentioned that the introduction of the particle-size distribution does not improve the quality of description, which serves as confirmation for the high monodispersity of the studied particles.

These results lead us to the thought that we are facing here not with the temperature transition of strongly magnetic particles into the superparamagnetic state, but with macroscopic quantum effects of repopulation of the particles' energy levels with different values of the magnetic moment, that have being often observed in nanoparticles of weakly magnetic materials and have recently found a theoretical explanation [4–6], and that the samples under study are, contrary to the initial expectations, an antiferromagnetic phase of trivalent iron oxide or hematite α-Fe_2O_3. This modification, exhibiting similar value of isomer shift and slightly greater hyperfine field, is characterized by quadrupolar interaction, which strongly varies with particles size ($q = 0.5 \ldots 0.2$ for mean diameters of about $4 \ldots 20$ nm) and only for bulk material undergoes Morin transition at 263 K, when EFG changes its orientation in the crystal [9]. Next sections of this work are dedicated to verification of our assumption.

3 Analysis in the quantum model

Vanishing of relaxation established by the preliminary analysis is rather natural for the ensemble of antiferromagnetic particles, since the dipole–dipole interactions between their total magnetic moments are smaller by several orders of magnitude than in ferro- and ferrimagnets. It is therefore worth to create a theory of antiferromagnetic particles that though ignores magnetic dynamics but involves specific thermodynamics of such systems. The most universal way of doing this is based on the quantum-mechanical representation of a problem with two macrospins of magnetic sublattices S_1 and S_2 coupled by exchange interaction and located in a magnetic anisotropy field [4, 5]. We use here its simplest variant for the case of equivalent spins $S_1 = S_2 = S$ [4], thus the Hamiltonian of the antiferromagnetic particle can be written as

$$\hat{H} = \frac{A}{S(S+1)} \left[\hat{\mathbf{S}}_1 \hat{\mathbf{S}}_2 - \frac{k}{2} \left(\hat{S}_{z1}^2 + \hat{S}_{z2}^2 \right) \right] \tag{6}$$

where $A$is the exchange coupling constant ($A > 0$), $\hat{\mathbf{S}}_{1,2}$ are the operators of the macrospins of sublattices, $\hat{S}_{z\,1,2}$ are the operators of their projections on the anisotropy axis, and $k = K/A$. Calculations in this model represent a solution of the complete eigenvalues problem in the basis of functions ψ_{m_1,m_2}, each characterized by a pair of projections $m_{1,2} = -S, \ldots, S$ of the spins of sublattices onto the anisotropy axis. Due to the axial symmetry of the Hamiltonian wave functions $\Psi_j^{(m)}$ corresponding to different total projections $m = m_1 + m_2$ are orthogonal, which factorizes the problem and allows to go to the secular equations

$$\hat{H} \left| \Psi_j^{(m)} \right\rangle = E_j^{(m)} \left| \Psi_j^{(m)} \right\rangle, \tag{7}$$

where $j = 1, \ldots, 2S + 1 - m$, and $E_j^{(m)}$ are the eigenvalues for the j-th state with a given m value. The simplicity of the calculations is also due to the tridiagonal form of the density matrices representing operators (7) in the basis of functions ψ_{m_1,m_2}.

The results of data processing in the quantum model of thermodynamics are presented in Fig. 2, and corresponding values of parameters are placed in Table 2. Let us first note the satisfactory agreement between the theory and experiment as well as the similarity between the values of hyperfine parameters and those found from the preliminary analysis over the low- and intermediate-temperature range. On the other hand, the absence of relaxation leads to a notable transformation of the high-temperature curves, but the quality of their description remains quite satisfactory, while the shape of these curves itself partially explains the resolved magnetic structure which appears in the spectra at high temperatures. Moreover, due to the more rigid computational scheme, all the model parameters are now precisely determined from the experiment without any a priori fixation.

4 Analysis in the macroscopic (continual) model

The quantum-mechanical representation (6)–(7) allows us to find time-averaged characteristics of the studied systems and therefore to calculate observable values in any static research methods, e.g. in conventional Mössbauer experiment. At the same time dynamical characteristics of the system is of a great importance for such radiofrequency techniques as ferro- or antiferromagnetic resonances. To consider dynamic effects in ideal antiferromagnetic particles let us start with the simplest macroscopic representation involving two magnetic sublattices with magnetization vectors $\mathbf{M}_1$ and $\mathbf{M}_2$ ($M_1 = M_2 = M_0$) under the influence of the exchange and anisotropy fields [6]

$$E = J\mathbf{M}_1\mathbf{M}_2 - \frac{K}{2}(\cos^2\theta_1 + \cos^2\theta_2) \tag{8}$$

with renormalized exchange coupling constant $J = A/M_0^2$ and the angles θ_1 and θ_2 between the easy axis and the vectors $\mathbf{M}_1$ and $\mathbf{M}_2$. Equations of motion for the i-th magnetic sublattice then have the form

$$\dot{\mathbf{M}}_i = -\gamma \left[\mathbf{M}_i, \mathbf{H}_i^{(\mathrm{eff})}\right], \tag{9}$$

which describe precession in the intrinsic effective field

$$\mathbf{H}_i^{(\mathrm{eff})} = -\partial E/\partial \mathbf{M}_i, \tag{10}$$

where γ denotes the magnetomechanical ratio.

Under the assumption of the axial symmetry of the solutions, these equations define four normal modes of self-consistent and uniform precession of magnetization vectors around the easy axis of the particle. In the usual case when the anisotropy energy KV is small compared to exchange energy AV:

$$k << 1, \tag{11}$$

the excitation spectrum of two fundamental modes is qualitatively similar to the energy spectrum in the standard model of ferromagnetic particles (1) with nearly opposite orientations of magnetization vectors of the sublattices, whereas their precessional frequencies response to antiferromagnetic resonance in the zero external field:

$$\omega_{1,2} = \pm\omega_0 = \mp\gamma H_0 \equiv \mp\gamma\sqrt{H_A(2H_E + H_A)}, \tag{12}$$

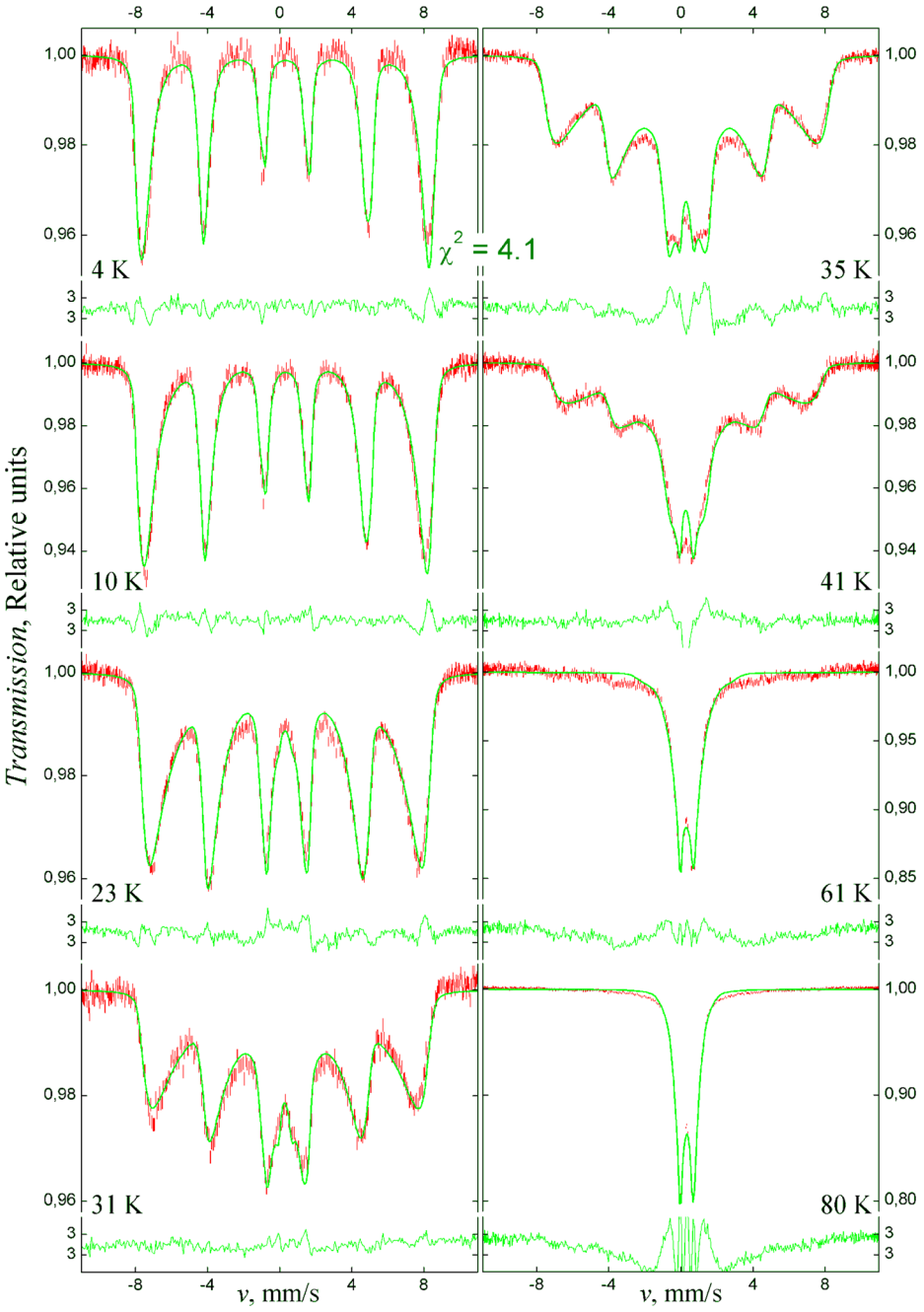

Fig. 2 Experimental (*red bars*) and theoretical (*green lines*) spectra calculated in the quantum-mechanical model of thermodynamics of antiferromagnetic particles

Table 2 Parameters of Fe_2O_3 nanoparticles, derived using the quantum-mechanical model of thermodynamics of antiferromagnetic particles: quadrupolar shift q and exchange energy AV shared for all temperatures, as well as anisotropy energy KV, hyperfine field H_{hf}, isomer shift δ and effective absorber thickness σ

T, K	4	10	23	31	35	41	61	80
q, mm/s	0.3525 (4)							
AV, K	180.0 (6)							
KV, K	38.9 (3)	75.2 (4)	99.9 (4)	91.4 (4)	80.9 (2)	60.5 (3)	15 (1)	12 (1)
H_{hf}, kOe	512.3 (2)	507.9 (2)	497.8 (2)	497.3 (5)	496.1 (3)	474.8 (9)	180 (4)	100 (1)
δ, mm/s	0.326 (3)	0.331 (2)	0.336 (2)	0.323 (5)	0.338 (2)	0.326 (4)	0.343 (2)	0.328 (1)
σ	2.80 (2)	3.07 (1)	2.91 (1)	2.61 (1)	2.92 (1)	2.80 (1)	2.29 (1)	2.491 (2)

where we use effective values of the exchange field $H_E = JM_0$ and anisotropy field $H_A = K/M_0$. At the same time the third branch, for which the normalized projections of the magnetization vectors onto the easy axis has the same value m_z, is characterized by the "exchange" frequency

$$\omega_3 = -\gamma H_E(2-k)m_z, \tag{13}$$

and it makes a comparable contribution to the spectrum only for the states with minor values m_z. The fourth mode, where vectors $\mathbf{M}_1$ and $\mathbf{M}_2$ coincide and precess with the ferromagnetic frequency

$$\omega_4 = \gamma H_A m_z, \tag{14}$$

lies much higher in terms of energy and plays no substantial role.

Nevertheless, modes of uniform precession (12)–(14), though giving principal explanation of the excitation spectrum of antiferromagnetic particles, are not enough for quantitative consonance with either experimental data or calculations in the quantum model (6)–(7), being only partial solutions of the equations (8–10). Their general solution may be obtained by the analogy with the problems about the nutations of a heavy gyroscope in the gravity field or about the swings of a pendulum out of its equilibrium plane [10], so as for the normalized longitudinal component l_z of the antiferromagnetic vector $\mathbf{L} = \mathbf{M}_1 - \mathbf{M}_2$ we have the following differential equation

$$dl_z = \pm\frac{\omega_0}{2}\sqrt{\left(l_z^2 - l_1(E,m)\right)\left(l_2(E,m) - l_z^2\right)}dt, \tag{15}$$

which depends on two integrals of motion: energy E and normalized projection m of the total magnetic moment $\mathbf{M} = \mathbf{M}_1 + \mathbf{M}_2$ onto the anisotropy axis. Functions l_1 and l_2 may be expressed in terms of algebraic roots of the biquadratic polynomials of m and define amplitude of nutations over the polar angle within all possible ranges of parameters variations. The exact calculation of the moments' trajectories upon the equation (15) is out of purposes of this paper and will be presented later on, but the averaged values of the moments may be expressed through the elliptic integral

$$I(\varepsilon) = \int_{\varepsilon}^{1} \frac{dx}{\sqrt{(x^2-\varepsilon^2)(1-x^2)}}, \tag{16}$$

where parameter ε is the combination of functions l_1 and l_2. Thus, all thermodynamic properties of an ensemble of antiferromagnetic particles are defined, and we may compute its static Mössbauer spectra.

The results of data analysis in the macroscopic model are presented in Fig. 3, and corresponding values of parameters are placed in Table 3. Their comparison with the results

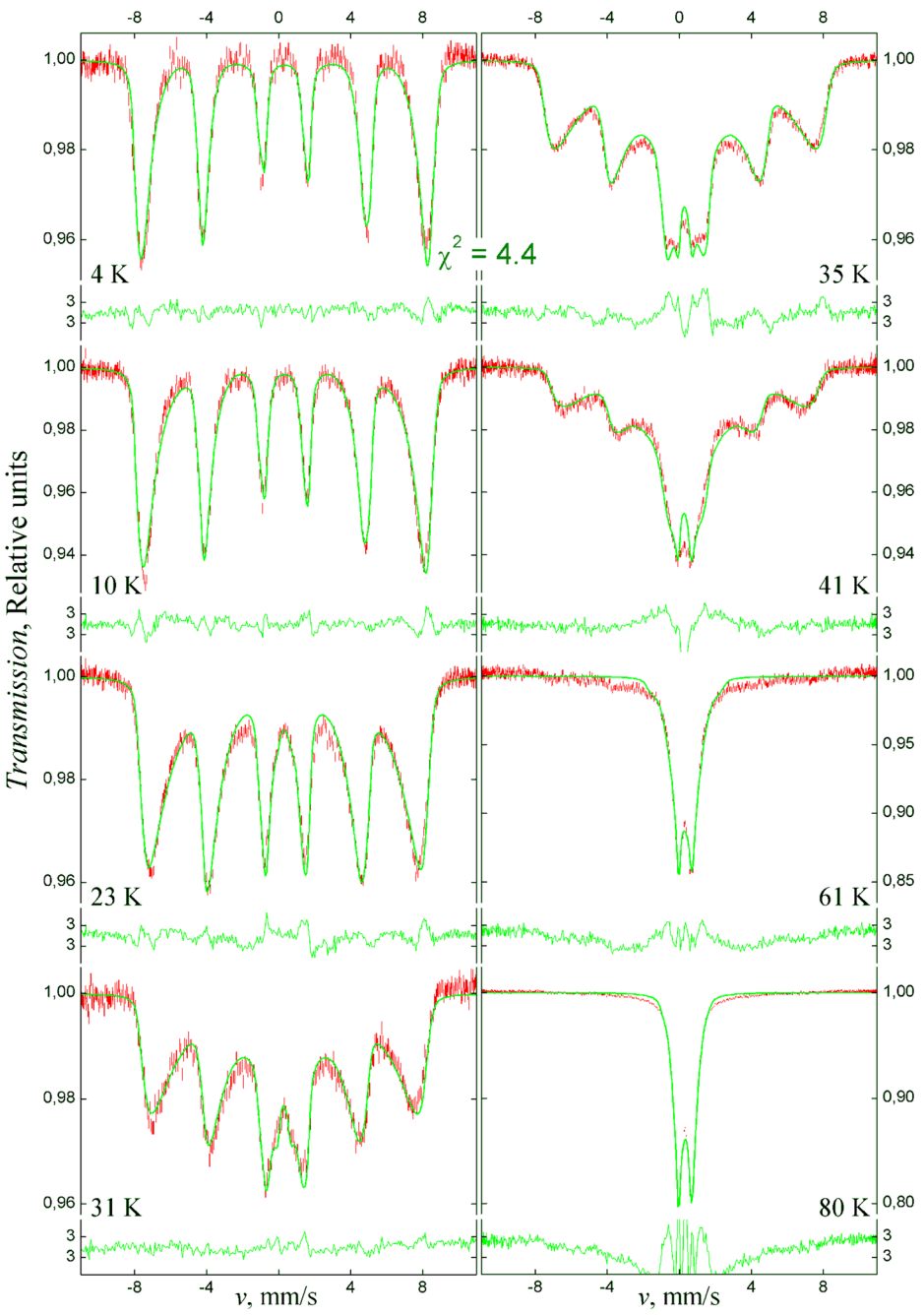

Fig. 3 Experimental (*red bars*) and theoretical (*green lines*) spectra calculated in the continual model of magnetic dynamics of antiferromagnetic particles

Table 3 Parameters of Fe_2O_3 nanoparticles, derived using the continual model of magnetic dynamics of antiferromagnetic particles and similar to those presented in Table 2

T, K	4	10	23	31	35	41	61	80
q, mm/s	0.3541 (4)							
AV, K	134.2 (4)							
KV, K	32.7 (6)	65.4 (6	85.0 (3)	79.5 (3)	71.4 (1)	55.1 (3)	32 (1)	35 (1)
H_{hf}, kOe	514.6 (5)	510.0 (3)	500.3 (2)	497.4 (5)	494.9 (3)	471.4 (9)	130 (2)	75 (1)
δ, mm/s	0.326 (3)	0.330 (2)	0.336 (2)	0.323 (5)	0.339 (2)	0.318 (4)	0.344 (2)	0.327 (1)
σ	2.85 (2)	3.10 (1)	2.91 (1)	2.61 (1)	2.89 (1)	2.76 (1)	2.23 (1)	2.458 (2)

in the quantum model shows that description of the experiment in both approaches is virtually identical, whereas optimum energy parameters are slightly different. This discrepancy probably originate from the constrain (11) which was used during the macroscopic consideration and is a bit tight for our case. Nevertheless, the concord of these two approaches with each other and with the results of the preliminary analysis of the low-temperature measurements is striking, which allows to consider these models as a reliable base for the further development of the analytical methods for nanomaterials diagnostics.

5 Conclusions

Comparatively simple physical approaches applied in this work may be generalized for accounting finer effects and for extracting more information about the studied systems. The most natural way for it is involving the uncompensated spin distribution, which does not change the main features of the description but makes it more realistic [5]. Another possibility consists in accounting other contributions to the anisotropy energy, besides those that originate from the form-factor of the particles, which can lead to better agreement between parameters restored at various temperatures.

At the same time, we believe that even the results obtained in the simplest physical models are the clear evidence of the antiferromagnetic behavior of the system under study. Some findings of the authors of [7], e.g. the weak saturation magnetization or the high resonant frequencies specific for antiferromagnetic samples (12)–(13), also confirm this hypothesis. However, the question about the magnetic ordering in ultrafine particles is by far not simple, and in order to judge confidently in this and in many other disputed cases, it is necessary not only to improve the models of antiferromagnets but also to develop a relevant theory of ferrimagnetic particles.

Acknowledgments We wish to thank Prof. J. Litterst and Dr. M. Kracken at the Technical University of Braunschweig for the experimental data. This work was supported by the Russian Foundation for Basic Research.

References

1. Jones, D.H., Srivastava, K.K.P.: Many-state relaxation model for the Mössbauer spectra of superparamagnets. Phys. Rev. B **34**, 7542–7548 (1986)

2. Chuev, M.A.: Multi-level relaxation model for describing the Mössbauer spectra of single-domain particles in the presence of quadrupolar hyperfine interaction. J. Phys.: Condens. Matter **23**, 426003(11pp) (2011)
3. Chuev, M.A.: Multi-level relaxation model for describing the Mössbauer spectra of nanoparticles in a magnetic field. J. Exp. Theor. Phys. **114**(4), 609–630 (2012)
4. Chuev, M.A.: Thermodynamics of antiferromagnetic nanoparticles and macroscopic quantum effects observed by Mössbauer spectroscopy. Proc. of SPIE. **8700**, 87000F (12pp) (2012)
5. Chuev, M.A.: Macroscopic quantum effects observed in Mössbauer spectra of antiferromagnetic nanoparticles. Hyperfine Interact **226**, 111–122 (2014)
6. Chuev, M.A.: Excitation spectrum and magnetic dynamics of antiferromagnetic nanoparticles in Mössbauer spectroscopy. JETP Lett. **99**(5), 278–282 (2014)
7. Bordonali, L., et al.: ^{1}H-NMR study of the spin dynamics of fine superparamagnetic nanoparticles. Phys. Rev. B **85**, 174426(7pp) (2012)
8. Bauminger, R., et al.: Study of the law-temperature transition in magnetite and the internal fields acting on iron nuclei in some spinel ferrites, using Mössbauer absorption. Phys. Rev **122**(5), 1447–1450 (1961)
9. Kündig, W., et al.: Some properties of supported small α-Fe_2O_3 particles determined by the Mössbauer effect. Phys. Rev **142**(2), 327–333 (1966)
10. Landau, L.D., Lifshitz, E.M.: Mechanics, 2nd edn., vol. 1. Pergamon Press, Oxford (1969)